Cell Reports, Volume *19*

Supplemental Information

Hepatocyte Hyperproliferation upon Liver-Specific Co-disruption of Thioredoxin-1, Thioredoxin Reductase-1, and Glutathione Reductase

Justin R. Prigge, Lucia Coppo, Sebastin S. Martin, Fernando Ogata, Colin G. Miller, Michael D. Bruschwein, David J. Orlicky, Colin T. Shearn, Jean A. Kundert, Julia Lytchier, Alix E. Herr, Åse Mattsson, Matthew P. Taylor, Tomas N. Gustafsson, Elias S.J. Arnér, Arne Holmgren, and Edward E. Schmidt

Supplemental Materials for:

Hepatocyte Hyperproliferation Upon Liver-specific Co-disruption of Thioredoxin-1, Thioredoxin Reductase-1 and Glutathione Reductase

Justin R. Prigge[1], Lucia Coppo[2], Sebastin S. Martin[2], Fernando Ogata[2], Colin G. Miller[1], Michael D. Bruschwein[1], David J. Orlicky[3], Colin T. Shearn[4], Jean A. Kundert[1], Julia Lytchier[2], Alix E. Herr[1], Åse Mattsson[2], Matthew P. Taylor[1], Tomas N. Gustafsson[2,5], Elias S. J. Arnér[2], Arne Holmgren[2], and Edward E. Schmidt[1]*

[1]Microbiology & Immunology, Montana State University, Bozeman, MT 59715 USA
[2]Division of Biochemistry, Medical Biochemistry & Biophysics, Karolinska Institutet, Stockholm SE-171 77 Sweden
[3]Department of Pathology, University of Colorado Anschutz Medical Center, Denver, CO 80045 USA
[4]Department of Pharmaceutical Sciences, University of Colorado Anschutz Medical Center, Denver, CO 80045 USA
[5]Department of Clinical Microbiology, Clinical Bacteriology, Sunderby Research Unit, Umeå University, SE-901 85 Umeå, Sweden

*Lead Contact. Please address correspondence to eschmidt@montana.edu

ph. (406) 994-6375
fx. (406) 994-4303

PO Box 173520
Montana State University
Bozeman, MT 59717 USA

Key words: thioredoxin, glutathione, methionine cycle, transsulfuration, ribonucleotide reductase, redox, proliferation, liver, mouse model, cancer.

DETAILED EXPERIMENTAL PROCEDURES

Mice and Surgeries

All mice were housed in the American Association for the Accreditation of Laboratory Animal Care (AAALAC)-accredited Animal Resources Center at Montana State University under specialized care conditions, including continuous-flow HEPA-filtered-air cages (Tecniplast); sterilized bedding and enrichment; unrestricted access to sterilized feed (Picolabs 5058 or 5053) and sterilized water; and on a 14:10 light:dark cycle. None of the experiments presented invovled fasting or other dietary modifications unless specifically indicated. Animal protocols were approved by the Montana State University Institutional Animal Care and Use Committee (MSU-IACUC). Wild-type C57Bl/6J mice, B6.Cg-Tg(Alb-cre)21Mgn/J mice bearing the "AlbCre" transgene (Postic et al., 1999), and *Gt(ROSA)26Sor*$^{tm4(ACTB-tdTomato,-EGFP)Luo}$/J mice (Muzumdar et al., 2007) bearing the Cre-responsive membrane-targeted, dual-fluorescent "*ROSA*$^{mT-mG}$" marker allele were obtained from The Jackson Laboratory (Bar Harbor, ME; stocks JAX#000664, JAX#003574, and JAX#007576, respectively). Mice bearing the *Gsr*$^{-}$ allele were kindly provided by L. Rogers (Rogers et al., 2004). Mice bearing the *Txnrd1*^{cond} (B6.129(Cg)-*Txnrd1*^{tm1Ees}/J, JAX#028283) (Bondareva et al., 2007), *Txnrd1*^{null}, and the Cre-responsive nucleus-targeted, dual-fluorescent "*ROSA*$^{nT-nG}$" (B6;129S6-*Gt(ROSA)26Sor*$^{tm1(CAG-tdTomato*,-EGFP*)Ees}$/J, JAX#023035) (Prigge et al., 2013) alleles, as well as *Txnrd1*$^{cond/cond}$*;AlbCre*$^{+}$ (AlbCre-driven liver-specific "TrxR1-null") (Suvorova et al., 2009) or *Txnrd1*$^{cond/cond}$*;Gsr*$^{-/-}$*;AlbCre*$^{+}$ (AlbCre-driven liver-specific "TrxR1/Gsr-null") (Eriksson et al., 2015) genotypes were described previously. Mice were genotyped by PCR using genomic DNA extracted from tail-biopsies harvested between postnatal day-10 (P10) and P14. All analyses shown were done on mice of both genders between P60 and P90, except as specifically noted in figure legends or text. In particular, the age-dependent ploidy analyses (Figure 6D in main text) used younger and older animals, and the acetaminophen toxicity analyses (Figure 5B in main text) used only males due to on published gender-specific sensitivities in mice (Iverson et al., 2013).

A conditional-null allele of the mouse *Txn1* gene in which exons 2-3 are flanked by codirectional *lox*P sites (*Txn1*^{fl}) was generated and targeted into embryonic stem (ES) cells. For targeting vector generation, PCR reactions used Phusion polymerase (New England Biolabs #M0531S) and were sequence-verified at all critical regions and junctions. The targeting vector used a region of the *Txn1* gene from chromosome 4 (Chr4) positions 57,954,765 - 57,948,263, which was amplified from Fosmid WI1-1371-M22 (BacPac Resource Center). Restriction endonuclease sites *Not* I and *Xho* I were engineered onto the amplified *Txn1* fragment at the 5' and 3' ends, respectively. *lox*P sites were inserted into introns 1 and 3 at Chr4 positions 57,952,026 and 57,950,650, respectively. The *lox*P site in intron 1 was flanked on its 5' end by an engineered *Pac* I site and replaced Chr4 endogenous sequences 57,952,027 - 57,952,032. The *lox*P site in intron 3 was flanked on its 5' end with an engineered *Asc* I site, and replaced Chr4 endogenous sequence 57,950,651 - 57,950,656. A self-excising frt-Prm1pFlpe-Pol2pNeo-frt cassette containing the region from *Sal* I to *Bgl* II (bases 1227 - 5969) of the FnF11 plasmid (Wu et al., 2008) was inserted into intron 2 at Chr4 position 57,951,056. The completed *Txn1* targeting sequence was inserted between *Not* I and *Xho* I sites in the TK1-TK2c plasmid (Thomas et al., 1986) and linearized with *Not* I prior to electroporation into male F1-C57Bl/6 x 129SvEvTac hybrid ES cells. Targeted ES cell clones were identified by PCR analysis on genomic DNA using primer pair *Txn1* intron 1-forward (5'-gctcagtgcttcacagaccacgt-3') and Prm1p-reverse (5'-ggaagctgaaaggtggacag-3'). One targeted ES cell clone was used to make chimeric mice in C57Bl/6J recipient blastocysts carrying the *Txn1*^{founder} allele. Phenotypically male chimeras were bred to C57Bl/6J females and pups were screened for self-excision of the Prm1pFlpe-Pol2pNeo cassette. Genotypes of mice carrying the unrecombined *Txn1*^{founder} allele or the Flpe-recombined *Txn1*^{fl} allele were determined using primer pairs *Txn1* intron 2-forward (5'-tatggatccagcacccaaatgggagagtca-3') and Prm1p-reverse, or *Txn1* intron 2-forward and *Txn1* intron 2-reverse (5'-tatgaattcaaaccaagaagcgttagaactgg-3'), respectively. Genomic DNA from F_1 *Txn1*$^{found/+}$ or *Txn1*$^{+/+}$ pups was amplified with primers flanking the D4mit193 polymorphism (D4mit193-forward, 5'-ctgcagcacttgatattgtcagt-3' and D4mit193-reverse, 5'-agaaaagacatacaattgatccacagg-3'), which showed that the *Txn1*^{found} allele was targeted to the C57Bl6/J chromosome in the hybrid F1-C57Bl/6 x 129SvEvTac hybrid ES cells. *Txn1*$^{fl/+}$ mice were interbred and genotypes of pups were determined using primer pair *Txn1* intron 2-forward and *Txn1* intron 2-reverse (5'-tatgaattcaaaccaagaagcgttagaactgg-3'). Total RNA harvested from *Txn1*$^{+/+}$, *Txn1*$^{fl/+}$, or *Txn1*$^{fl/fl}$ livers was used to make oligo (dT)-primed cDNA and Trx1 mRNA expression was analyzed using primer pair *Txn1* exon 1-forward (5'-tatgaattcatggtgaagctgatcgagagca-3') and *Txn1* exon 5-reverse (5'-tatgtcgactcagatggcagttgggtatagact-3'). Mice bearing the *Txn1*^{fl} allele are publicly available from Jackson Labs (stock JAX#030221). *Txn1*^{fl} and AlbCre were subsequently combined with *Txnrd1*^{cond} (Bondareva et al., 2007) and *Gsr*^{null} (Rogers et al., 2004). Mice with TrxR1-, Gsr-, Trx1-, TrxR1/Gsr-, Trx1/TrxR1-, Trx1/Gsr-, and Trx1/TrxR1/Gsr-null livers are all overtly normal as adults and fertile in both genders. Mice with triple-null livers have lived over a year as breeders before being retired.

Hepatic ischemia/reperfusion (I/R) injury surgeries (Jaeschke, 2003) were performed by a modification of the 2/3 hepatectomy procedure we have used previously (Eriksson et al., 2015; Mitchell and Willenbring, 2008; Rollins et al., 2010). Briefly, once the liver was exposed and the membrane was cut between the median and left lateral lobes of isofluorane/O_2-anesthetized mice, a non-traumatic clamp was applied near the base of the left lateral lobe. This occluded circulation to ~1/3 of the liver, which was immediately evident as a change in coloration of the ischemic lobe. The open body cavity was then covered with a sterile saline-wetted gauze and maintained on a warmed table under isofluorane/O_2 anesthesia with constant monitoring. After 30 min of ischemia, the clamp was removed and the body wall and skin were closed. Mice were monitored twice daily for development of any adverse signs and harvested 14 d after surgery. Samples from the left lateral (ischemic) and median (non-ischemic) lobes were separately harvested for histological analyses.

Acetaminophen challenge was performed as described previously (Iverson et al., 2013). Briefly, acetaminophen in sterile saline was administered by I.P. injection to all animals at the indicated concentrations at 8:30-9:00 am and animals were harvested 24 h later.

Tissue Harvests, Histology, and Sample Preparation

Mice were sacrificed by isofluorane inhalation, weighed, and livers were perfused with sterile saline (cardiac-portal) prior to removal. For analysis of serum markers, blood (~0.7 - 1.4 ml) was collected from the inferior vena cava immediately upon harvest by syringe using a 23 ga. needle, and serum was prepared using Sarstedt Microvette tubes. Snap-frozen serum was sent on dry ice to Marshfield Laboratories (Marshfield, Wisconsin) for analysis on "Veterinary Hepatic Panel 2".

For electron microscopy, livers were perfused (cardiac-portal) immediately upon sacrifice with normal saline followed by 10% neutral-buffered formalin. Livers were then removed and ~ 1 mm^3 cubes were cut with a sharp razor. Tissue cubes were fixed in Carnoy's fixative, embedded in Spurr's medium, thin-sectioned, and stained as described previously (Iverson et al., 2013). Images were digitally captured at 5000X magnification on a Zeiss LEO-912 transmission electron microscope. For other analyses, harvested whole liver was weighed and ~ 250 mg samples were snap-frozen in liquid nitrogen for protein/enzyme analyses or were fixed in neutral-buffered formalin for histology. Histological samples were embedded in paraffin, sectioned (5 µm thickness), and stained with hematoxylin and eosin (H&E) by standard procedures (Iverson et al., 2013). Horseradish peroxidase (HRP)-based immunostaining for phosphohistone-H3 (PHH3) and proliferative cell nuclear antigen (PCNA), including antigen retrieval, was performed as described previously using paraffin-embedded sections (Prigge et al., 2012; Rollins et al., 2010). Primary antibodies were mouse-anti-PCNA (AbCam #A1029) or rabbit-anti-PHH3 or rabbit-anti-Ki-67 (Cell Signaling Technology #9701 or #D3B5, respectively). HRP conjugated secondary antibodies for immunostaining were goat-anti-mouse (Pierce #31430), goat-anti-rabbit (GIBCO #13859.012), or, for Ki-67 staining, SignalStain Boost IHC Detection Reagent (Cell Singaling Technology #8114). Chromogen Tablets (Diagnostic Biosystems #K001) were used for color development. For immunohistochemical detection of protein-4-HNE adducts using an antibody raised in-house (Shearn et al., 2015), protein acrolein adducts (Cell Sciences #PA2049) (Shearn et al., 2013), or protein-SSG (Virogen #101-A-100) (Shearn et al., 2016), the Vectastain ABC kit (Vector Labs) was used with citrate (pH 6.0) antigen retrieval. Histologic images were captured on an Olympus BX51 microscope equipped with a four-megapixel Macrofire digital camera (Optronics) using the PictureFrame Application 2.3 (Optronics).

For enzymatic and immunblotting analyses, fragments (~100 mg) of frozen liver were pulverized under liquid nitrogen with a mortar and pestle. Powdered liver was transferred to Eppendorf tubes and thawed by the addition of ~5 volumes of homogenization buffer (50 mM Tris-HCl, pH 7.5; 150 mM NaCl; 2 mM EDTA; 1% Triton X-100; 1X protease inhibitor cocktail [Roche #11697498001], at 4^{o}C). Samples were further homogenized in a glass-glass Dounce homogenizer (A-pestle) on ice and were clarified by centrifugation at full-speed in a table-top microcentrifuge for 10 min at 4°C. Supernatant was collected and stored in aliquots at -80°C. Protein concentration was determined using a Bradford assay (Bio-Rad #5000001) with BSA to generate a standard curve.

Immunoblotting

Immunoblots used 20 µg of total protein of the clarified lysate from the indicated samples per lane, boiled in 1X loading dye (Bio-Rad #1610747) supplemented with final concentration of 7 mM DTT prior to running, except when analyzing Prx2, for which the DTT was omitted. For immunoblots, antibodies were as follows: anti-TrxR1 and

anti-Trx1, rabbit antisera raised against recombinant mouse proteins, kindly provided by G. Merrill, Oregon State University, and each used at 1:4000 dilutions; anti-human Gsr (conserved oligopeptide epitope), mouse monoclonal (Santa Cruz Biotechnology, #sc-133136) used at 1:1000; anti-human Trx2 (conserved oligopeptide epitope) rabbit polyclonal antiserum, (Santa Cruz Biotechnology, #sc-50336), used at 1:1000 dilution; rabbit-anti-mouse Glrx1 antibody, affinity purified (IMCO, Inc.), used at 1:500 dilution; anti-TRP14 rabbit antiserum raised against full-length recombinant mouse protein for this study, used at 1:2000 dilution; anti-mouse Prx2, rabbit polyclonal antiserum (AbFrontier # LF-PA0091) used at 1:1000 dilution; mouse anti-b-Actin (conserved oligopeptide epitope) monoclonal antibody (Sigma-Aldrich #A5441). Secondary antibodies for immunoblotting were goat-anti-mouse-HRP or goat-anti-rabbit-HRP (Santa Cruz Biotechnology, #sc-2005 or #sc-2030, respectively), and were used at 1:5000 dilutions. Proteins were visualized by chemiluminescence using the ECL system (GE Healthcare #RPN2016).

Enzymatic Assays

Total glutathione levels were determined using the GSH-recycling assay (Rahman et al., 2006) as described previously (Eriksson et al., 2015). Briefly, clarified protein lysates were acidified by adjusting to 1% sulfosalicylic acid and after 5 min of incubation at 4 °C, the samples were centrifuged 10 m, 10,000 x g, 4°C, and 10 µl of each sample, corresponding to 30 µg of protein lysate, was mixed with a solution of 5,5′-dithiobis(2-nitrobenzoic acid) (DTNB; 1.68 mM) and yeast Gsr (Sigma-Aldrich, #G9297; 2.4 U/ml) in 0.1 M potassium phosphate buffer, pH 7.4, 5 mM EDTA. After 30 s, NADPH (0.8 mM final concentration; VWR #80053-342) was added and the rate of production of GSH was determined by the change in absorbance at 412 nm. Gsr activity was measured as described using 30 µg of protein lysate with the Gsr activity analysis kit (Cayman Chemical #703202; Figure 1I) or by measuring the production of free thiols via colorimetric conversion DTNB (Figure 1J). For the later, 225 µl reaction mixtures of 100 mM phosphate buffer (pH 7.5), 1 mM EDTA, containing 70 µg of liver lysate and 200 µM of either NADH or NADPH, and 1 mM GSSG, as indicated, were incubated at 37^{o}C. Reactions were stopped immediately or after 1h by adding 500 µl of a solution of 6M guanidine-HCl and 1 mM DTNB, and absorbance was read at 415 nm. Values from zero-time controls were subtracted from the 1 h values. Grx activity was measured on 20 µg of protein lysates using and IMCO fluorescent assay kit (FkGRX-01)(Coppo et al., 2016).

Measurements of mitochondrial enzymatic activities were performed on liver samples that had been saline-perfused at harvest and snap-frozen in liquid nitrogen prior to shipment on dry ice to the University of Alabama at Birmingham Bio-Analytical Redox Biology Core facility. Briefly, kinetic assays were measured on a DU800 spectrophotometer using 15 µg of protein from each sample. Complex I activity was immediately measured at 600 nm using 2,6-dichloroindophenol (DCIP) as the terminal electron acceptor and the oxidation of NADH reducing artificial substrate Coenzyme Q10 that then reduced DCIP (Janssen et al., 2007). Complex II activity was analyzed as the reduction of dichloroindophenol at 600 nm with succinate as the substrate, and complex II/III was measured as the reduction of cytochrome *c* at 550 nm, also using succinate as the substrate (Spinazzi et al., 2012). Complex III was measured by reduction of cytochrome c at 550 nm at 30^{o}C. The reaction was initiated by adding 75 µM reduced decylubiquinone (DUBQH2), and the increase in absorbance at 550nm was measured for 3 min. Rates were calculated from the linear portion of the trace and the specific complex III activity was calculated (Spinazzi et al., 2012). Complex IV activity was measured by the oxidation of cytochrome c at 550 nm and data are represented as the pseudo first order rate constant (k) divided by protein concentration (Brink et al., 1987). ATP synthase (Complex V) activity was measured by the continuous spectrophotometric monitoring of the oxidation of NADH (e340 = 6180 $M^{-1}cm^{-1}$) in an enzyme-linked ATP regenerating assay using ATP, phosphoenolpyruvate, pyruvate kinase, and lactate dehydrogenase to determine the ATPase activity (NADH loss) in µmol/min/mg protein (Feniouk et al., 2007; Pullman et al., 1960). Citrate synthase was measured by the coupled reaction with oxaloacetate, acetyl-CoA, and 5,5-dithiobis-(2,4-nitrobenzoic acid)(Hoppeler, 1986; Leek et al., 2001; Shepherd and Garland, 1969).

Establishment of Primary Fibroblast Cultures, *Ex Vivo* Conversion of Floxed Alleles, and Analyses Using Fibroblast Cultures

All cultured cells were grown on standard plastic tissue culture dishes or multi-well plates in a humidified water-jacketed incubator at 37^{o}C in ambient air using "standard" cell culture medium, consisting of DMEM (GIBCO #31885 or the equivalent, which includes 5.6 mM D-glucose, 4.0 mM L-glutamine, and 1.0 mM sodium pyruvate; all components diluted to ~88% concentration by serum and antibiotic additions in final medium); supplemented

with 10% FCS and 1X penicillin/streptomycin (Sigma 15140122); and further modified or supplemented as indicated in figures or legends. Procedures for establishing and Cre-converting mouse primary fibroblast cultures were as we have described previously (Suvorova et al., 2009). Briefly, biopsies were taken from adult mouse ears that had been surface-disinfected sequentially with 70% ethanol, betadine solution, and 70% ethanol. Biopsies in sterile saline were minced with a scissors or razor blade. Cells were dispersed with 2X trypsin/EDTA solution (diluted from 10X stock into sterile saline, ThermoFisher #15400) and seeded onto 10 cm tissue culture dishes containing 10 ml of standard medium. When cultures reached confluence, they were split onto 2 dishes. These were grown to confluence and frozen stocks were prepared.

For ex vivo conversion, cultures re-established from frozen stocks were grown to ~90% confluence on 10 cm dishes. Cells were lifted with 1X trypsin/EDTA, washed 1X with standard medium, dispersed in 100 µl of standard medium, and then inoculated with 10 µl of a ~10^9 PFU/ml stock of AdCre (Suvorova et al., 2009). Cells were incubated at room temperature with intermittent gentle mixing for 10 m and then seeded either onto 10 cm dishes for immunoblotting or dispersed into the wells of a 6- or 12-well dish pre-incubated with standard medium (one AdCre-treated 10 cM dish used to seed all wells of a single multi-well dish), which resulted in all wells being fully confluent at the 0 h time-point. For immunoblots, cells were rinsed 1X with PBS, harvested by scraping in ice-cold 1X PBS, pelleted, and lysed by sonication followed by boiling in 1% SDS, 10 mM Tris, pH 7.5, 5 mM EDTA. Protein concentrations were determined by bicinchoninic acid analyses (Sigma BCA-1) and 20 µg of each was assayed per lane. As indicated, cultures were treated with 3 mM L-buthionine-(S,R)-sulfoximine (BSO, ACROS 235520050), 3 mM D,L-propargylglycine (PPG, Sigma P7888), or with an additional 28 mM D-glucose ("hyperglycemic stress"; final concentration ~33 mM) at 4 d post AdCre inoculation. After 48 h of challenge, cells on dishes were gently rinsed 3X with 1X PBS to remove dead cells and were photographed under phase-contrast on an inverted microscope. For quantification, adherent live cells were counted on 10- to 20-fields of view under each condition.

Morphometry

For morphometric analyses of hepatocytes and hepatocyte nuclei, digital images of 5 µm-thick H&E-stained paraffin sections from adult livers were photographed under uniform conditions using a 20X objective. The area of whole individual hepatocytes and their respective nuclei were measured by pixel-counts using the Histogram function in Adobe Photoshop CS3 software. Only hepatocytes that had nuclei in the plane of section and had clearly defined membrane margins were analyzed, and the plane of section on all measured objects was assumed to be equatorial. Experimenter supervision was used to ensure that representative frequencies of hepatocytes of all sizes and morphologies were presented in data sets. Analyses were done on >25 hepatocytes from each of 3 different liver sections from each three to five animals per genotype. For visibly bi-nucleate hepatocytes, it was assumed that both nuclei were equal size and, if one was smaller in a given image, the larger one was assumed to be in the plane of section, and the measurement of this nucleus was used for both nuclei. All hepatocytes that had only one nucleus in the plane of section were assumed to be mono-nucleate. To convert the data into relative volumetric estimates, we assumed that each measured object was an ovoid of the maximal and minimal radial dimensions viewed in the plane of section, and thus the area (pixel-count) of each object was squared. Since this protocol was followed for all images, intrinsic error is uniform for each group and genotype-specific differences are representative.

For measuring the sizes of mitochondria in transmission electron micrographs, images taken at 5000X magnification were analyzed for area using ImageJ 1.51h software (National Institutes of Health). Total cytoplasmic area in each frame was determined by subtracting nuclear and extracellular area from each image. For each genotype, 10 to 25 arbitrary fields of view were analyzed, containing a total of 140, 105, 345, 135, 210, 158, and 387 individual mitochondria in WT, TrxR1-, Trx1-, TrxR1/Gsr-, Trx1/TrxR1-, Trx1/Gsr-, and Trx1/TrxR1/Gsr-null hepatocytes, respectively. All morphometric data were tabulated, analyzed, and plotted using GraphPad Prism 7 software.

Statistical Analyses

Statistical analyses were performed using Excel or GraphPad Prism 7 software. Bar graphs show means and s.e.m. values and significance was determined by paired Student's T-tests versus values for control (wild-type) samples.

References for Supplemental Section

Bohm, N., and Noltemeyer, N. (1981). Development of binuclearity and DNA-polyploidization in the growing mouse liver. Histochemistry *72*, 55-61.

Bondareva, A.A., Capecchi, M.R., Iverson, S.V., Li, Y., Lopez, N.I., Lucas, O., Merrill, G.F., Prigge, J.R., Siders, A.M., Wakamiya, M., et al. (2007). Effects of thioredoxin reductase-1 deletion on embryogenesis and transcriptome. Free Radic Biol Med *43*, 911-923.

Brink, J., Hovmoller, S., Ragan, C.I., Cleeter, M.W., Boekema, E.J., and van Bruggen, E.F. (1987). The structure of NADH:ubiquinone oxidoreductase from beef-heart mitochondria. Crystals containing an octameric arrangement of iron-sulphur protein fragments. Eur J Biochem *166*, 287-294.

Coppo, L., Montano, S.J., Padilla, A.C., and Holmgren, A. (2016). Determination of glutaredoxin enzyme activity and protein S-glutathionylation using fluorescent eosin-glutathione. Anal Biochem *499*, 24-33.

Eriksson, S., Prigge, J.R., Talago, E.A., Arner, E.S., and Schmidt, E.E. (2015). Dietary methionine can sustain cytosolic redox homeostasis in the mouse liver. Nature communications *6*, 6479.

Feniouk, B.A., Suzuki, T., and Yoshida, M. (2007). Regulatory interplay between proton motive force, ADP, phosphate, and subunit epsilon in bacterial ATP synthase. J Biol Chem *282*, 764-772.

Griffith, O.W., and Meister, A. (1985). Origin and turnover of mitochondrial glutathione. Proc Natl Acad Sci U S A *82*, 4668-4672.

Hoppeler, H. (1986). Exercise-induced ultrastructural changes in skeletal muscle. Int J Sports Med *7*, 187-204.

Iverson, S.V., Eriksson, S., Xu, J., Prigge, J.R., Talago, E.A., Meade, T.A., Meade, E.S., Capecchi, M.R., Arner, E.S., and Schmidt, E.E. (2013). A Txnrd1-dependent metabolic switch alters hepatic lipogenesis, glycogen storage, and detoxification. Free Radic Biol Med *63*, 369-380.

Jaeschke, H. (2003). Molecular mechanisms of hepatic ischemia-reperfusion injury and preconditioning. Am J Physiol Gastrointest Liver Physiol *284*, G15-26.

Janssen, A.J., Trijbels, F.J., Sengers, R.C., Smeitink, J.A., van den Heuvel, L.P., Wintjes, L.T., Stoltenborg-Hogenkamp, B.J., and Rodenburg, R.J. (2007). Spectrophotometric assay for complex I of the respiratory chain in tissue samples and cultured fibroblasts. Clinical chemistry *53*, 729-734.

Kombu, R.S., Zhang, G.F., Abbas, R., Mieyal, J.J., Anderson, V.E., Kelleher, J.K., Sanabria, J.R., and Brunengraber, H. (2009). Dynamics of glutathione and ophthalmate traced with 2H-enriched body water in rats and humans. American journal of physiology. Endocrinology and metabolism *297*, E260-269.

Leek, B.T., Mudaliar, S.R., Henry, R., Mathieu-Costello, O., and Richardson, R.S. (2001). Effect of acute exercise on citrate synthase activity in untrained and trained human skeletal muscle. American journal of physiology. Regulatory, integrative and comparative physiology *280*, R441-447.

Meister, A. (1991). Glutathione deficiency produced by inhibition of its synthesis, and its reversal; applications in research and therapy. Pharmacol Ther *51*, 155-194.

Meister, A., and Griffith, O.W. (1979). Effects of methionine sulfoximine analogs on the synthesis of glutamine and glutathione: possible chemotherapeutic implications. Cancer treatment reports *63*, 1115-1121.

Meister, A., Griffith, O.W., Novogrodsky, A., and Tate, S.S. (1979). New aspects of glutathione metabolism and translocation in mammals. Ciba Found Symp, 135-161.

Meredith, M.J., and Reed, D.J. (1982). Status of the mitochondrial pool of glutathione in the isolated hepatocyte. J Biol Chem *257*, 3747-3753.

Mitchell, C., and Willenbring, H. (2008). A reproducible and well-tolerated method for 2/3 partial hepatectomy in mice. Nat Protoc *3*, 1167-1170.

Muzumdar, M.D., Tasic, B., Miyamichi, K., Li, L., and Luo, L. (2007). A global double-fluorescent Cre reporter mouse. Genesis *45*, 593-605.

Ohtsubo, K., and Nomaguchi, T.A. (1986). A flow cytofluorometric study on age-dependent ploidy class changes in mouse hepatocyte nuclei. Mech Ageing Dev *36*, 125-131.

Postic, C., Shiota, M., Niswender, K.D., Jetton, T.L., Chen, Y., Moates, J.M., Shelton, K.D., Lindner, J., Cherrington, A.D., and Magnuson, M.A. (1999). Dual roles for glucokinase in glucose homeostasis as determined by liver and pancreatic beta cell-specific gene knock-outs using Cre recombinase. J Biol Chem *274*, 305-315.

Prigge, J.R., Eriksson, S., Iverson, S.V., Meade, T.A., Capecchi, M.R., Arner, E.S., and Schmidt, E.E. (2012). Hepatocyte DNA replication in growing liver requires either glutathione or a single allele of txnrd1. Free Radic Biol Med *52*, 803-810.

Prigge, J.R., Wiley, J.A., Talago, E.A., Young, E.M., Johns, L.L., Kundert, J.A., Sonsteng, K.M., Halford, W.P., Capecchi, M.R., and Schmidt, E.E. (2013). Nuclear double-fluorescent reporter for in vivo and ex vivo analyses of biological transitions in mouse nuclei. Mamm Genome *24*, 389-399.

Pullman, M.E., Penefsky, H.S., Datta, A., and Racker, E. (1960). Partial resolution of the enzymes catalyzing oxidative phosphorylation. I. Purification and properties of soluble dinitrophenol-stimulated adenosine triphosphatase. J Biol Chem *235*, 3322-3329.

Rahman, I., Kode, A., and Biswas, S.K. (2006). Assay for quantitative determination of glutathione and glutathione disulfide levels using enzymatic recycling method. Nat Protoc *1*, 3159-3165.

Rogers, L.K., Tamura, T., Rogers, B.J., Welty, S.E., Hansen, T.N., and Smith, C.V. (2004). Analyses of glutathione reductase hypomorphic mice indicate a genetic knockout. Toxicol Sci *82*, 367-373.

Rollins, M.F., van der Heide, D.M., Weisend, C.M., Kundert, J.A., Comstock, K.M., Suvorova, E.S., Capecchi, M.R., Merrill, G.F., and Schmidt, E.E. (2010). Hepatocytes lacking thioredoxin reductase 1 have normal replicative potential during development and regeneration. J Cell Sci *123*, 2402-2412.

Severin, E., Meier, E.M., and Willers, R. (1984). Flow cytometric analysis of mouse hepatocyte ploidy. I. Preparative and mathematical protocol. Cell Tissue Res *238*, 643-647.

Shearn, C.T., Orlicky, D.J., McCullough, R.L., Jiang, H., Maclean, K.N., Mercer, K.E., Stiles, B.L., Saba, L.M., Ronis, M.J., and Petersen, D.R. (2016). Liver-Specific Deletion of Phosphatase and Tensin Homolog Deleted on Chromosome 10 Significantly Ameliorates Chronic EtOH-Induced Increases in Hepatocellular Damage. PLoS One *11*, e0154152.

Shearn, C.T., Orlicky, D.J., Saba, L.M., Shearn, A.H., and Petersen, D.R. (2015). Increased hepatocellular protein carbonylation in human end-stage alcoholic cirrhosis. Free Radic Biol Med *89*, 1144-1153.

Shearn, C.T., Smathers, R.L., Backos, D.S., Reigan, P., Orlicky, D.J., and Petersen, D.R. (2013). Increased carbonylation of the lipid phosphatase PTEN contributes to Akt2 activation in a murine model of early alcohol-induced steatosis. Free Radic Biol Med *65*, 680-692.

Shepherd, D., and Garland, P.B. (1969). The kinetic properties of citrate synthase from rat liver mitochondria. Biochem J *114*, 597-610.

Spinazzi, M., Casarin, A., Pertegato, V., Salviati, L., and Angelini, C. (2012). Assessment of mitochondrial respiratory chain enzymatic activities on tissues and cultured cells. Nat Protoc *7*, 1235-1246.

Suvorova, E.S., Lucas, O., Weisend, C.M., Rollins, M.F., Merrill, G.F., Capecchi, M.R., and Schmidt, E.E. (2009). Cytoprotective Nrf2 pathway is induced in chronically txnrd 1-deficient hepatocytes. PLoS One *4*, e6158.

Thomas, K.R., Folger, K.R., and Capecchi, M.R. (1986). High frequency targeting of genes to specific sites in the mammalian genome. Cell *44*, 419-428.

Wu, S., Ying, G., Wu, Q., and Capecchi, M.R. (2008). A protocol for constructing gene targeting vectors: generating knockout mice for the cadherin family and beyond. Nat Protoc *3*, 1056-1076.

Table S1. Mitochondrial Activity Assays, Related to Figure 4

	CX1 µm/min/mg	**CX2** nm/min/mg	**CX3** nm/min/mg	**CX4** k/sec/mg*	**CX5** µm/min/mg	**Cs** mU/mg
WT	215.5	39.4	390.8	6.19	247.8	102.8
n=3, (SEM)	(89.1)	(8.5)	(75.8)	(2.16)	(5.8)	(5.9)
TrxR1/Gsr-null	335.2	38.9	446.0	4.42	206.0	92.0
n=3, (SEM)	(19.7)	(9.2)	(26.3)	(0.34)	(9.8)	(8.7)
[*P*]	[0.261]	[0.968]	[0.529]	[0.465]	[**0.021**]	[0.294]
Trx1/TrxR1-null	281.1	52.9	469.2	3.15	206.8	131.0
n=3, (SEM)	(30.0)	(9.3)	(102.6)	(0.95)	(14.2)	(11.2)
[*P*]	[0.521]	[0.345]	[0.571]	[0.267]	[0.055]	[0.754]
Trx1/Gsr-null	271.2	27.2	456.6	8.65	214.0	99.7
n=3, (SEM)	(42.1)	(11.2)	(55.3)	(3.44)	(30.0)	(4.65)
[*P*]	[0.603]	[0.437]	[0.522]	[0.577]	[0.330]	[0.142]
Trx1/TrxR1/Gsr-null	300.9	24.0	336.0	2.95	187.5	87.3
n=3, (SEM)	(46.0)	(4.4)	(38.5)	(0.93)	(17.5)	(6.3)
[*P*]	[0.444]	[0.182]	[0.555]	[0.240]	[**0.031**]	[0.210]

*Data for CX4 are presented as the pseudo first order rate constant per protein concentration, see Materials and Methods. Abbreviations: Cs, citrate synthase; CX1-5, electron transport chain complexes I - V; [*P*], Student's T-test versus WT. n, number of animals. Each measurement was performed at least 3 times on each animal. **Red bold font**, $P < 0.05$.

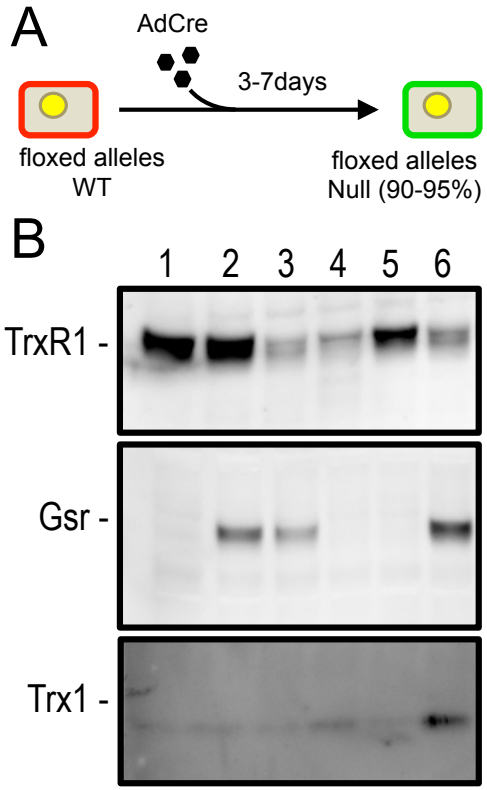

Figure S1. Primary fibroblast model for assessing combinatorial genetic disruptions of Trx1, TrxR1, and Gsr, Related to Figure 2

A. Schematic.

B. Fibroblast gene conversion. Protocols followed those published previously (Suvorova et al., 2009). Primary fibroblast cultures were initiated from ear biopsies taken from mice harboring various combinations of Gsr^{null}, $Txnrd1^{cond}$, and $Txn1^{fl}$, in addition to being homozygous for the Cre-responsive dual-fluorescent $ROSA^{mT-mG}$ allele (Muzumdar et al., 2007). Cells were grown on 10 cm tissue culture dishes in DMEM containing 1 mg/l glucose, 2 mM glutamine, 1 mM pyruvate, and supplemented with 10% fetal calf serum, and 1X penicillin + streptomycin, in a 5% CO_2 37°C incubator. Near-confluence cells were lifted off dishes with trypsin, rinsed with complete medium, pelleted, and resuspended in 0.5 ml complete medium/10^6 cells. To this, 10 µl of ~10^9 plaque-forming units/ml adenoviral-Cre vector (AdCre)(Suvorova et al., 2009) was added (MOI ~ 10^1), cells were incubated at room temperature with gentle mixing for 10 m, and were seeded either onto fresh 10 cm dishes for immunoblot analyses or onto fresh dishes or wells. By 72 h after AdCre exposure, most cells were visibly green under fluorescence microscopy and immunoblots (e.g., shown here) indicated that levels of TrxR1 and Trx1 protein had decayed to ~10% of initial levels. These levels did not change at 5-, or 7-day time points (not shown), suggesting they represented the frequency of cells or alleles on the dish that escaped Cre-mediated recombination. Genotypes of the mice from which the primary fibroblasts were initiated were: (lane 1) $Txnrd1^{+/+};Gsr^{-/-};Txn1^{fl/fl};ROSA^{mT-mG/mT-mG};AlbCre^{1}$ [converted culture Trx1/Gsr-null]. (lane 2) $Txnrd1^{+/+};Gsr^{+/+};Txn1^{fl/fl};ROSA^{mT-mG/mT-mG};AlbCre^{1}$ [converted culture Trx1-null]. (lane 3) $Txnrd1^{cond/cond};Gsr^{-/+};Txn1^{fl/fl};ROSA^{mT-mG/mT-mG};AlbCre^{1}$ [converted culture TrxR1/Trx1-null; Gsr-heterozygous]. (lane 4) $Txnrd1^{cond/cond};Gsr^{-/-};Txn1^{fl/fl};ROSA^{mT-mG/mT-mG};AlbCre^{1}$ [converted culture Txr1/TrxR1/Gsr-null]. (lane 5) $Txnrd1^{cond/+};Gsr^{-/-};Txn1^{fl/fl};ROSA^{mT-mG/mT-mG};AlbCre^{1}$ [converted culture TrxR1-heterozygous; Trx/Gsr-null]. (lane 6) $Txnrd1^{cond/cond};Gsr^{+/+};Txn1^{+/+};ROSA^{mT-mG/mT-mG};AlbCre^{1}$ [converted culture TrxR1-null]. Most cultures showed robust survival; however Trx1/TrxR1/Gsr-null cultures started exhibiting cells releasing from the dish after day-8 post-AdCre. Based on these observations, stress-challenges were initiated at 96 h post AdCre and were terminated 48 h later.

Prigge et al., 2017, **Supplemental Figure S2**

A. Estimated volume of 4N hepatocyte

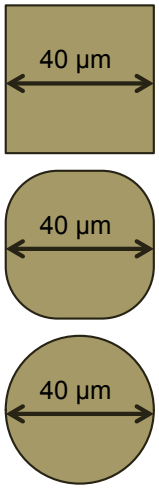

V = (40 µm)^3 = 64,000 µm^3 = 64 pl

V (estimate) = 50,000 µm^3 = 50 pl

V = 4/3 π (20 µm)^3 = 33,500 µm^3 = 33.5 pl

B. Hepatocyte GSH content versus DNA content

1) 5 mM GSH = 5 fmol/pl
2) 5 fmol/pl x 50 pl/4N hepatocyte = 250 fmol/4N hepatocyte
3) 250 fmol = 15 x 10^{10} molecules GSH
4) Synthesis of 1 DNA base requires 1 electron-pair = 2 GSH
5) 1N = 2.72 x 10^9 base pairs = 5.44 x 10^9 DNA bases
6) 4N = 2.18 x 10^{10} DNA bases; replication of 4N hepatocyte requires 4.4 x 10^{10} electrons
7) 4.4 x 10^{10} electrons required/15 x 10^{10} GSH = 29%
8) Conclusion: Hepatocytes contain a steady state concentration of GSH with sufficient electrons to replicate their entire genome ~ 3 times

C. Kinetic requirement for GSH biosynthesis to support replication in a 4N hepatocyte

1) Based on a 2 h GSH half-life, at steady state GSH synthesis is 3.8 x 10^{10} molecules/h in 4N hepatocytes
2) S phase in a 4N hepatocyte is ~ 7 h and requires 4.4 x 10^{10} electrons (= 4.4 x 10^{10} molecules of GSH)
3) During S phase, hepatocytes need 0.63 x 10^{10} electrons/hour for DNA synthesis (= 0.63 x 10^{10} GSH/h)
4) Therefore, the rate of electron consumption for S phase in a hepatocyte is only ~6% of the rate of GSH turnover in resting hepatocytes.

Figure S2. Estimation of Hepatocyte GSH Content and GSH Requirements, Related to Figure 6.

A. Hepatocyte volume estimation. In adult mice, the average ploidy of a hepatocyte is ~4N (Bohm and Noltemeyer, 1981; Ohtsubo and Nomaguchi, 1986; Prigge et al., 2013; Severin et al., 1984), so measurements and calculations here are based on a 4N average genome content. Average hepatocyte shape was approximated by a "rounded cube", with a long side of 30-40 µm, which was estimated to be intermediate between the volume of a cube with 40 µm sides and the volume of a sphere with a 20 µm radius, or ~50 pl.

B. Hepatocyte GSH and DNA content. The concentration of GSH in liver cytosol is reported to be ~5 mM (Meister and Griffith, 1979; Meister et al., 1979) and the haploid mouse DNA content is 2.72 x 10^9 base pairs (Mouse Genome Initiative). Based on these values and a 50 pl volume for a tetraploid hepatocyte (panel A), the hepatocyte contains ~3-fold more electrons in the steady state GSH pool than would be required by RNR to replicate the entire tetraploid genome.

C. Relative GSH requirements for DNA replication versus other processes. The half-life of GSH in liver have been reported to lie between ~0.2 and 2 h (Griffith and Meister, 1985; Kombu et al., 2009; Meister, 1991; Meredith and Reed, 1982). Thus, the rate of GSH biosynthesis to maintain steady state is at least 10-fold greater than the rate of additional GSH production that would be needed to support S phase in cells that could only fuel RNR through *de novo* synthesis of GSH, such as within TrxR1/Gsr-null livers (Eriksson et al., 2015).

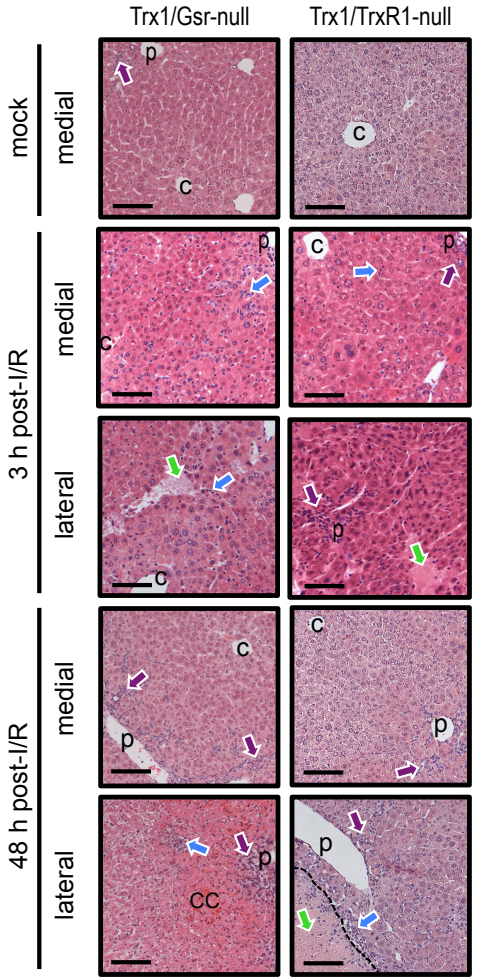

Figure S3. Early Pathology in Post-I/R-injury Livers, Related to Figure 5
Representative histology is shown from livers of genotypes Trx1/TrxR1- and Trx1/Gsr-null livers following either mock-I/R injury or either 3 h or 48 h after I/R-injury. In all cases, the left lateral lobe (lateral) was subjected to I/R and the medial lobe was unmanipulated. Green arrows denote necrotic cells or acellular post-necrotic debris, with a large necrotic zone outlined in dashed lines in bottom-left panel. Blue and purple arrows denote representative inflammatory cells or ductular reactions, respectively. Abbreviations: c, central vein; SC, sinusoidal congestion; p, portal triad. Scale bars, 100 μm.

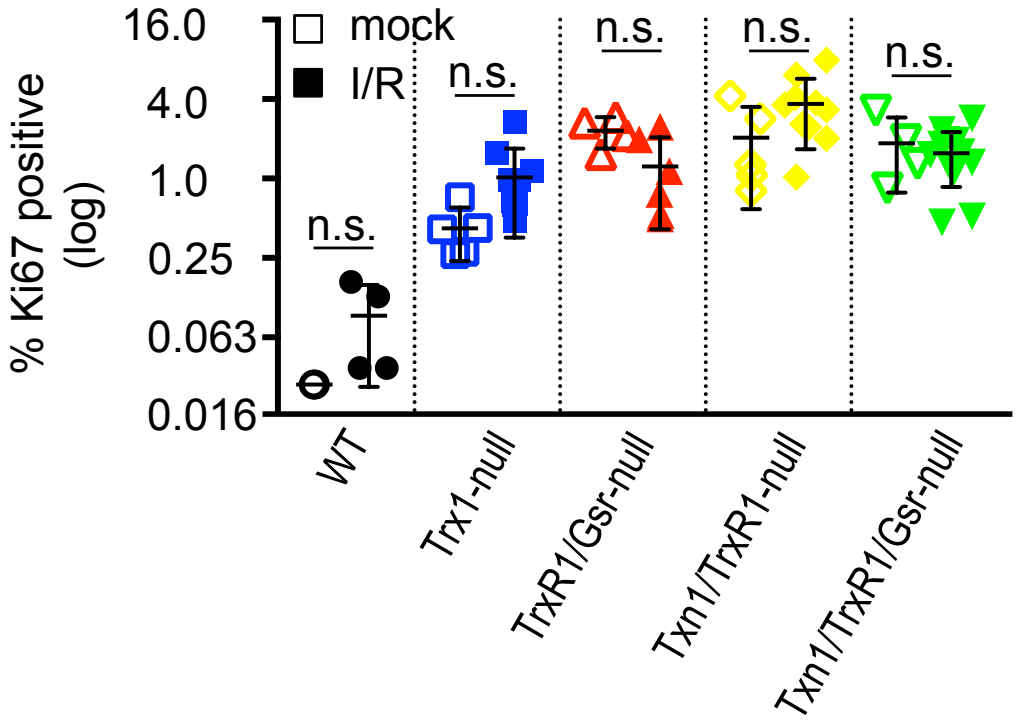

Figure S4. Ki-67 Staining on Post-I/R-injury Livers, Related to Figures 5 and 6

Paraffin sections of mouse livers harvested 2 weeks after I/R-injury were stained for Ki-67 antigen and photographed at 200X magnification. For post-I/R animals, samples from the lateral (ischemic) and medial (non-ischemic) lobes were analyzed separately. At this time point there were no significant differences between these lobes and a separate data point for each is included in the graph. The frequency of stained (proliferative) cells was tabulated on 30 fields of view for each mock-I/R animal, and on 30 fields of view from each analyzed lobe for each I/R-injury animal. Data points show the mean value for each animal, and bars depict the mean and standard deviation for all animals of each condition. The number of animals (n) represented for mock-I/R surgery is 3, 5, 4, 5, and 4 for WT, Trx1-, TrxR1/Gsr-, Trx1/TrxR1-, and Trx1/TrxR1/Gsr-null genotypes, respectively. For I/R-surgery groups, n = 4, 5, 3, 5, 6 in the same order of genotypes.